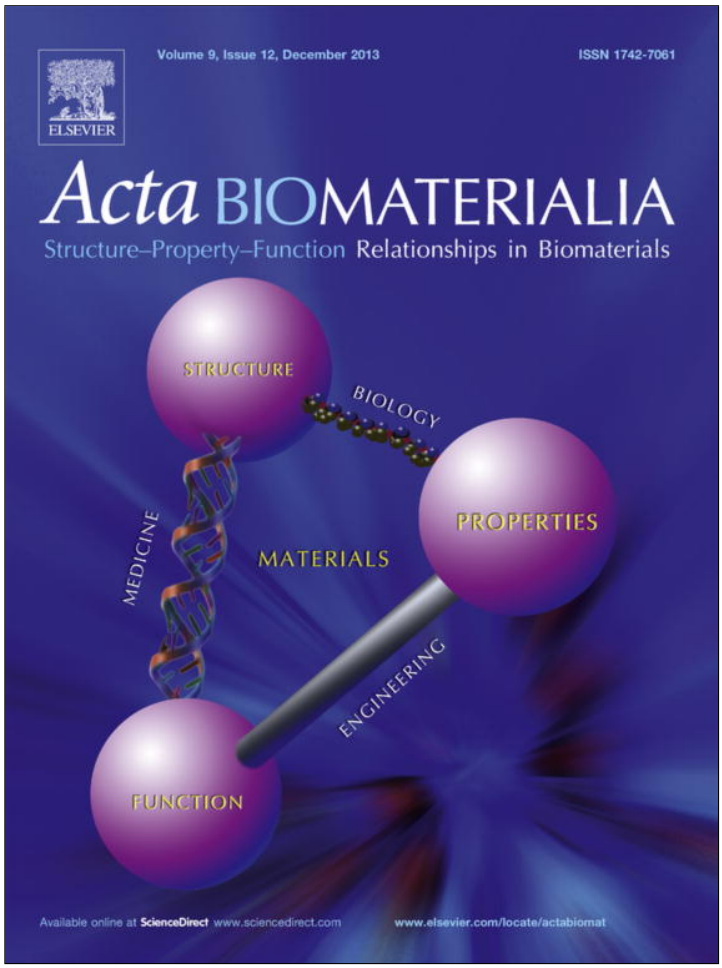

Acta Biomaterialia 9 (2013) 9351–9359

Contents lists available at ScienceDirect

Acta Biomaterialia

journal homepage: www.elsevier.com/locate/actabiomat

# Dual growth factor releasing multi-functional nanofibers for wound healing

Zhiwei Xie [a,b], Christian B. Paras [b], Hong Weng [b], Primana Punnakitikashem [b], Lee-Chun Su [b], Khanh Vu [b], Liping Tang [b], Jian Yang [a,*], Kytai T. Nguyen [b,*]

[a] Department of Bioengineering, Materials Research Institute, The Huck Institutes of the Life Sciences, The Pennsylvania State University, University Park, PA 16802, USA
[b] Department of Bioengineering, The University of Texas at Arlington, Arlington, TX 76019, USA

ARTICLE INFO

*Article history:*
Received 19 April 2013
Received in revised form 8 July 2013
Accepted 24 July 2013
Available online 2 August 2013

*Keywords:*
Wound healing
Nanofibers
Nanoparticles
Dual-release
Growth factors

ABSTRACT

The objective of this research is to develop a dual growth factor-releasing nanoparticle-in-nanofiber system for wound healing applications. In order to mimic and promote the natural healing procedure, chitosan and poly(ethylene oxide) were electrospun into nanofibrous meshes as mimics of extracellular matrix. Vascular endothelial growth factor (VEGF) was loaded within nanofibers to promote angiogenesis in the short term. In addition, platelet-derived growth factor-BB (PDGF-BB) encapsulated poly(lactic-co-glycolic acid) nanoparticles were embedded inside nanofibers to generate a sustained release of PDGF-BB for accelerated tissue regeneration and remodeling. In vitro studies revealed that our nanofibrous composites delivered VEGF quickly and PDGF-BB in a relayed manner, supported fibroblast growth and exhibited anti-bacterial activities. A preliminary in vivo study performed on normal full thickness rat skin wound models demonstrated that nanofiber/nanoparticle scaffolds significantly accelerated the wound healing process by promoting angiogenesis, increasing re-epithelialization and controlling granulation tissue formation. For later stages of healing, evidence also showed quicker collagen deposition and earlier remodeling of the injured site to achieve a faster full regeneration of skin compared to the commercial Hydrofera Blue® wound dressing. These results suggest that our nanoparticle-in-nanofiber system could provide a promising treatment for normal and chronic wound healing.



## 1. Introduction

Wound healing is a dynamic, complex, multicellular process involving extracellular matrix (ECM), cytokines, blood cells and many other factors [1]. Due to the pathological and physiological complexity of the wound healing process, perfect tissue regeneration is difficult to achieve [2]. This is especially true for chronic wounds, which affect millions of patients and have the associated cost of ~US$20 billion annually in the USA; hence progress of new treatment strategies or methodologies is greatly needed [3]. Traditional wound dressing normally acts as a temporary barrier for hemostasis and infection prevention purposes [4]. In recent decades, natural and synthetic skin grafts have been developed for replacement applications. However, most of them are expensive, require extensive care and do not regain full skin functionalities [5]. Hydrogel is another candidate for the wound treatment with benefits of maintaining moisture at the wound site and capability of drug delivery [6]. However, most hydrogels are non-degradable and difficult to use for large wounds [7]. To date, current treatment methods failed to achieve satisfaction of regaining barrier functionality and the cosmetic appearance of natural skin [8].

Using growth factors and their combinations in vivo has been suggested as a promising treatment to promote active healing [9,10]. However, until now, only platelet-derived growth factor-BB (PDGF-BB) has successfully completed clinical trials [11]. One of the major obstacles is that growth factors are either easily degraded by proteinases [12] or removed by exudate before reaching the wound bed [13]. Recent effort has been made on delivering growth factors via electrospun fibers for diabetic wound healing applications [14–16]. Compared to other wound dressing formations, electrospun nanofibers provide an ECM-like scaffold to support skin regeneration [17,18]. However, without a fundamental understanding of the biological process and better administration techniques to release biological molecules at essential points of the healing process, optimal wound healing having a fast and finely orchestrated nature still remains a challenge [19,20].

Normally, skin wound healing shows three overlapping phases: initial inflammation, tissue regeneration to fill the wound bed and tissue remodeling to regain skin functionalities. Recent developments discovered that during each phase of the dynamic process,

* Corresponding authors. Tel.: +1 8148651278; fax: +1 8148630490 (J. Yang). Tel.: +1 8172722540; fax: +1 8172722251 (K.T. Nguyen).
*E-mail addresses:* jxy30@psu.edu (J. Yang), knguyen@uta.edu (K.T. Nguyen).

1742-7061/$ - see front matter © 2013 Acta Materialia Inc. Published by Elsevier Ltd. All rights reserved.
http://dx.doi.org/10.1016/j.actbio.2013.07.030

many cytokines and growth factors are critical to modulate various cellular processes, including hemostasis, cell migration, differentiation, ECM formation, angiogenesis, and so on [1,2]. Some of the most important factors, like epidermal growth factors (EGFs), platelet-derived growth factor (PDGF), transforming growth factor (TGF-β), vascular endothelial growth factor (VEGF) and fibroblast growth factor (FGF-2), present at different healing stages with certain functionalities [21]. For example, VEGF is a key mediator for angiogenesis and granulation tissue formation in the early stage of healing [21,22]. On the other hand, PDGF is crucial for inflammation, granulation, re-epithelialization and remodeling throughout the three phases of wound healing [1,21].

In this study, we intended to create a biomimetic system that could serve as scaffold to support wound healing while releasing VEGF and PDGF-BB in a relayed manner to simulate the angiogenesis and cell proliferation at various phases, thereby facilitating the wound healing process. The optimal goal will be creating an integration of biochemical stimulation, cell growth support and bacteria inhibition that promotes favorable cell behaviors in skin wounds. Electrospinning is used to fabricate nanofiber composites containing chitosan, poly(ethylene oxide), VEGF and nanoparticles, which are loaded with PDGF-BB. Unlike existing research that uses either electrospun fibers with antibacterial nanoparticles [23] or antibiotics [24,25], the anti-infection issue is addressed on the fiber itself in this work. It is well-known that chitosan is an antibacterial polymer [26]. We hypothesize that introducing VEGF in the early stage could promote new blood vessel formation and sequentially bring more nutrition and oxygen to the wound site, and providing PDGF-BB throughout the whole process will facilitate the wound healing. Thus, a relatively fast release is required for VEGF, which will be released from electrospun fibers; and a sustained release is critical for PDGF-BB, which will be released from polymeric nanoparticles within the fibers. Our unique device could provide a structural mimic of ECM and anti-infection behavior, and supply specific growth factors when they are necessary to synergistically improve the complex wound healing treatment.

## 2. Materials and methods

### 2.1. Materials

Chitosan (CS, medium molecular weight, 75–85% deacetylated), poly(ethylene oxide) (PEO, Mn: 600,000 Dalton), acetic acid, chloroform and other chemicals were purchased from Sigma Aldrich (St Louis, MO). Poly-lactic-co-glycolic acid (PLGA) (50:50) was purchased from Lakeshore Biomaterials (Birmingham, AL). PDGF-BB and vascular endothelial growth factor (VEGF) were purchased from Prospec (East Brunswick, NJ). Adult human dermal fibroblast (HDF) cells were purchased from ATCC (Manassas, VA). Gram-negative *Escherichia coli* (*E. coli* 25922) and gram-positive *Staphylococcus aureus* (*S. aureus* 25923) were also obtained from ATCC. All other chemicals if not specified were purchased from Sigma Aldrich (St Louis, MO).

### 2.2. Fabrication of PLGA nanoparticles

PLGA nanoparticles fabrication was carried out using the double-emulsion technique as previously described [27]. Briefly, 200 μl 2% w/v PDGF-BB solution was added to 3.33 ml 3% w/v PLGA solution and sonicated at 30 W for 2 min. This o/w solution was then added dropwise to 12 ml 2% PVA solution and sonicated at 20 W for 2 min. Final w/o/w solution was de-solvated overnight using a magnetic stirrer. Centrifugation was then performed for 4,000 rpm for 5 min to get rid of particle aggregates. The PDGF-BB loaded PLGA nanoparticles were washed and collected using ultracentrifugation, and then further obtained via freeze-drying. In addition, the supernatant from the nanoparticle formation process was also collected to determine the loading efficiency as previously reported [27].

### 2.3. Fabrication nanofibers via electrospinning

The CS stock solution was prepared at a concentration of 2.5% w/v CS in 90% acetic acid. PEO solution at 8% w/v was prepared in DI water at room temperature. Two CS/PEO blend solutions were prepared by mixing the two stock solutions at 1:1 and 2:1 chitosan to PEO volume ratios (in this study, nanofibers without nanoparticles/growth factors were named as 1:1 CS/PEO and 2:1 CS/PEO). In another experiment, 20 wt.% of PLGA nanoparticles to PEO weight was sonicated into the mixture CS/PEO solution for 10–15 min at 20 W for complete dispersion of the nanoparticles (nanofibers with nanoparticles loaded with VEGF and PDGF-BB were named as 2:1 CS/PEO-NPs).

For electrospinning, the blended solutions were loaded into 5 ml syringe and fitted with an 18-gauge blunt needle tip. The solution feed was driven using a syringe pump at a flow rate of 1.5 μl $min^{-1}$, and a 15 cm distance and DC voltage of 18 kV were applied between the collector (aluminum mesh) and needle. All experiments were carried out at ambient temperature and relative humidity of 15–20%.

### 2.4. Characterization of fiber meshes

The surface morphology of the electrospun nanofiber mesh was characterized using a scanning electron microscope (SEM; Hitachi, S-3000N). All samples were first sputter-coated by silver. Fiber diameters were also determined using Image-J software. For each mesh, 100 fibers were considered from three different images to calculate the average diameter. To visualize the nanoparticles within the nanofibers, indocyanine green (ICG) loaded PLGA nanoparticles were prepared and electrospun. Fluorescent images were taken using fluorescent microscopy with a TRITC filter.

### 2.5. In vitro growth factor release from electrospun fiber meshes

To assess the growth factor release kinetics, VEGF was loaded in CS/PEO nanofibers, while PDGF-BB was encapsulated in the PLGA nanoparticle that embedded in the scaffolds. The scaffolds weighing 10.0–11.0 mg were loaded into 100 kDa dialysis membranes and placed in the 0.1 M PBS solution with pH 7.4. Samples were then placed on an orbital shaker at 37 °C. At predetermined time points, 1 ml of PBS solution was collected, stored at −20 °C for later analysis, and replenished with 1 ml fresh PBS. The release profiles of VEGF and PDGF-BB were analyzed using ELISA following the manufacturer's instructions (Invitrogen, Carlsbad, CA). Loading efficiency of VEGF was determined by dissolving the nanofibers in PBS and following with ELISA. Loading efficiency of PDGF-BB was determined indirectly by measuring the PDGF-BB concentration in washing solutions collected in the nanoparticle formation process by ELISA. Cumulative release over a period of 3 days was performed on all samples.

### 2.6. In vitro cell proliferation

Adult human dermal fibroblasts (HDFs) (passage numbers up to 10) were cultured in complete Dulbecco's modified Eagle's medium (DMEM) with supplements of 10% fetal bovine serum (FBS) and 1% penicillin/streptomycin. Cells were sub-cultured until ~80% confluency and maintained at a humidified atmosphere of 95% air and 5% $CO_2$. For in vitro cell proliferation on nanofiber meshes, scaffold samples (3 mm diameter) were vacuum dried

overnight and then UV-sterilized for 1 h. Samples were then placed in a 96-well plate and seeded with 5000 cells per well. Tissue culture plate (TCP) was used as control. MTS assays were performed at time points of 1, 3, 5 and 7 days following the manufacturer's instructions. PDGF-BB PBS solution (free PDGF-BB) was also used as a positive control. At each time point, 5 ng $ml^{-1}$ PDGF-BB was added into each well of TCP. Cell proliferation was plotted over time by percentage over the TCP control at each time point, which is normalized into 100% to observe the effects of growth factors on cell growth.

### 2.7. Antibacterial assessment of nanofiber meshes

To assess the antibacterial activity of the nanofibrous samples, three types of nanofiber scaffolds, including 1:1 CS/PEO, 2:1 CS/PEO and 2:1 CS/PEO-NPs, were used. All scaffold samples were vacuum-dried and UV sterilized, and ~20 mg of each scaffold type were used. *E. coli* and *S. aureus* were reconstituted based on product instruction for this study. Briefly, 1 ml of broth was added to rehydrate the bacterium pellet, and then a few drops of the suspension was mixed with 10 ml broth and incubated on an orbital shaker at 37 °C overnight. Bacteria suspension and PEO nanofibers without chitosan were chosen as the negative controls. Penicillin–streptomycin (Penstrep) was chosen as the positive control. For each sample, bacterial suspension was prepared at an optical density (OD) of 0.011 at 600 nm (measured by a UV–vis spectrophotometer, diluted 50 times from the suspension that has an OD corresponding to McFarland Standard Solution #1, $\sim 5 \times 10^6$ CFU $ml^{-1}$), added to the sample and incubated at 37 °C. After incubation, absorbance at 600 nm of each sample was read at predetermined time points. Averages of background samples (broth without bacteria) were subtracted from bacterial samples and plotted over a time course. All operations were performed under aseptic conditions.

### 2.8. In vivo wound healing studies

Sprague–Dawley rats weighing ~250 g were used for in vivo full thickness skin wound healing studies. All animals were treated and used according to the protocol approved by the University of Texas at Arlington Animal Care and Use Committee (IACUC). Animals were anesthetized with ketamine (40 mg $kg^{-1}$) and xylazine (5 mg $kg^{-1}$), and then shaved on the back. A 5 mm diameter biopsy puncher was used to create a wound along the dorsal side of the skin. Four wounds were created on each rat (six rats were used for each time point), and then controls (open wound and Hydrofera Blue®) and samples of nanofiber meshes (2:1 CS/PEO) without growth factors and nanofiber meshes with nanoparticles and growth factors (2:1 CS/PEO-NPs) were placed on the wound site randomly. Changes in the wound areas were measured using a caliper at 1, 7, 14 and 28 days after initial wounding. At each time point, animals were euthanized by exposure to 100% $CO_2$, then the surrounding skin and muscle including wound areas were removed and fixed by 10% neutral buffed formalin. Tissue samples were embedded in paraffin and sectioned. Hematoxylin and eosin (H&E) and Masson's Trichrome staining were performed to evaluate the skin tissue sections. Physical measurements of surface epidermal tongue and granulation tissue thickness of the H&E images were made using Image-J (NIH). Collagen quantification was carried out by measuring the blue area percentage of the wound area (Masson's Trichrome staining) by using MATLAB (MathWorks).

### 2.9. Statistical analysis

All data are presented as the mean + standard deviation (SD). Statistical analysis of all data was performed using 1-way ANOVA (StatView) whereas $p$ values < 0.05 were considered statistically significant ($n = 6$).

## 3. Results and discussion

As a structural mimic of ECM, electrospun nanofibers have been recently studied for tissue engineering applications [17,28]. Recently, using electrospun fibers to deliver growth factors gained more research interest, since growth factor releasing scaffolds are able to promote cellular and biological activities, thereby facilitating wound healing and tissue regeneration [29,30]. In this study, a nanoparticle/nanofiber complex was prepared to deliver two growth factors with different releasing manners. The system was designed to simulate and accelerate the wound healing process, instead of just as a slow release system as developed earlier [31,32]. As illustrated in Fig. 1, PDGF-BB was encapsulated within PLGA nanoparticles (153 ± 36 nm in average diameters determined by dynamic light scattering), and then dispersed in chitosan/PEO nanofibers to achieve a sustained release. In the same setting, VEGF was loaded into the nanofibers to provide a rapid release of VEGF in order to promote angiogenesis in early stages of the healing process. This nanocomposite system was further investigated in vitro and in vivo for its potential use in wound healing applications, and the results will be discussed in detail in the next sections.

### 3.1. Morphology of the nanoparticle loaded nanofibers

Scanning electron microscope images (Fig. 2A and B) of electrospun CS/PEO-NPs scaffolds show smooth, uniform and bead-less fibrous nonwoven structure. 1:1 CS/PEO had a smaller average fiber diameter of 116 ± 39 nm while 2:1 CS/PEO has an average nanofiber diameter of 132 + 39 nm. The fiber diameter increased with increasing chitosan concentration, since polymer concentration is the dominant factor for electrospun fiber diameters [33]. On the other hand, fiber diameter distribution (Fig. 2D) indicates that 2:1 CS/PEO-NPs has a wide non-uniform diameter range compared to a more uniform fiber formation of 1:1 CS/PEO-NPs with most frequent diameters within 130–150 nm, suggesting that the more chitosan content, the less uniform the fiber formation when NPs are incorporated. In order to visualize the nanoparticles within fibers, PLGA nanoparticles were loaded with indocyanine green (ICG) and imaged by a fluorescent microscopy. As shown in Fig. 2C, we can see that nanoparticles were located within fibers and uniformly distributed. The morphology is similar to the result

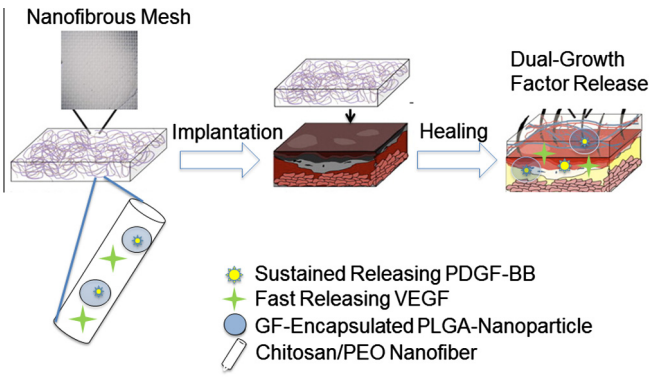


**Fig. 1.** Schematic illustration of the nanoparticle embedded electrospun nanofibers loaded with two growth factors for the wound healing. By applying these nanofiber/nanoparticle complexes on skin wound site, the chitosan/PEO nanofibers will act as a scaffold to support tissue regeneration, while fast releasing VEGF and slow releasing PDGF-BB will be the therapeutic agents that come into play at different healing stages.

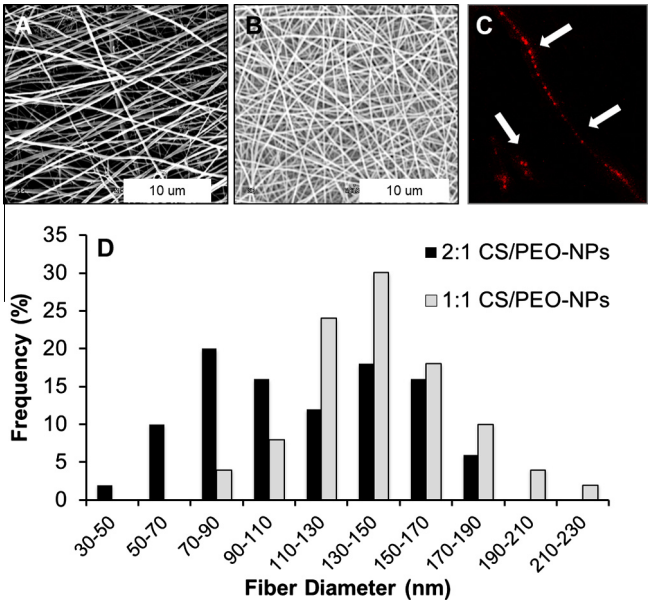


**Fig. 2.** Characterization of the nanoparticle embedded electrospun nanofibers. SEM images of nanofiber scaffolds: 2:1 CS/PEO-NPs (A) and 1:1 CS/PEO-NPs (B). Fluorescent image merges monochrome image of ICG-loaded NPs in CS/PEO fibers, as indicated by arrows (C). Diameter distribution of the nanoparticle embedded electrospun nanofibers (D).

of previous efforts that developed inorganic nanoparticle loaded electrospun fibers [34]; even our particles distinguished themselves by biodegradable polymer composition.

### 3.2. Controlled releasing profile

Using gradually releasing growth factors as a "cocktail" treatment has been suggested as an effective approach for complex wound healing [8]. Previous effort was based on layer-by-layer assembly [35,36] and core–shell electrospinning [37] to achieve two drugs releasing in different manners. However, the diffusion between layers still remains a critical problem [38]. Therefore, our nanoparticle-in-fiber system could serve as an alternative strategy and be able to endow a "fast and slow" biphasic release for two different growth factors.

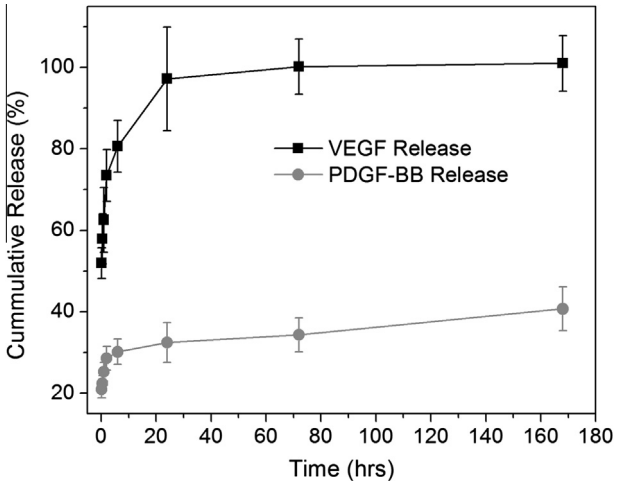


**Fig. 3.** Growth factor release kinetics from nanofibers and nanoparticles within fibers as determined by ELISA. VEGF was released from 1:1 CS/PEO-NPs nanofibers in PBS at 37 °C. PDGF-BB was release from PLGA nanoparticles encapsulated in 1:1 CS/PEO-NPs nanofibers under the same conditions.

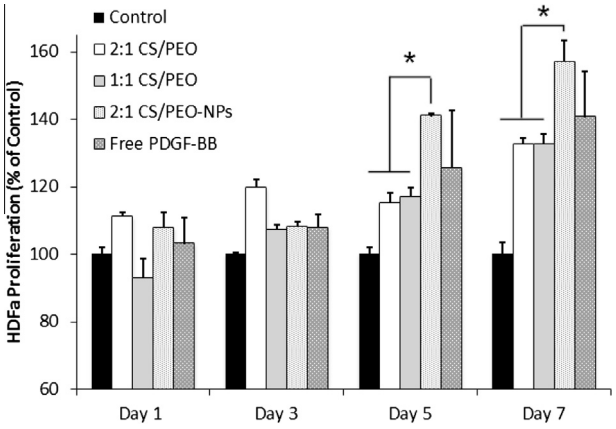


**Fig. 4.** Cell proliferation on nanofiber scaffolds: 1:1 CS/PEO, 2:1 CS/PEO without growth factors nanoparticles, 2:1 CS/PEO with PLGA nanoparticles loaded with PDGF-BB (2:1 CS/PEO-NPs). Tissue culture plate and free PDGF-BB were served as negative and positive controls, respectively. Nanofiber meshes and controls were seeded with adult human dermal fibroblast (HDFs) and MTS assay was used to quantify the cell viability ($^*p < 0.01$).

To determine the controlled growth factor release profile from our fibrous mesh, ELISA was performed. VEGF releases from CS/PEO nanofibers and PDGF-BB releases from nanoparticles embedded within nanofibers were measured and displayed in Fig. 3. VEGF released from nanofibers quickly showed that CS/PEO scaffold consisted of an initial burst release of 63% within 1 h. Also, the VEGF loaded within fibers of the CS/PEO scaffold reached almost 100% releases by day 1. In contrast, PDGF-BB released from PLGA

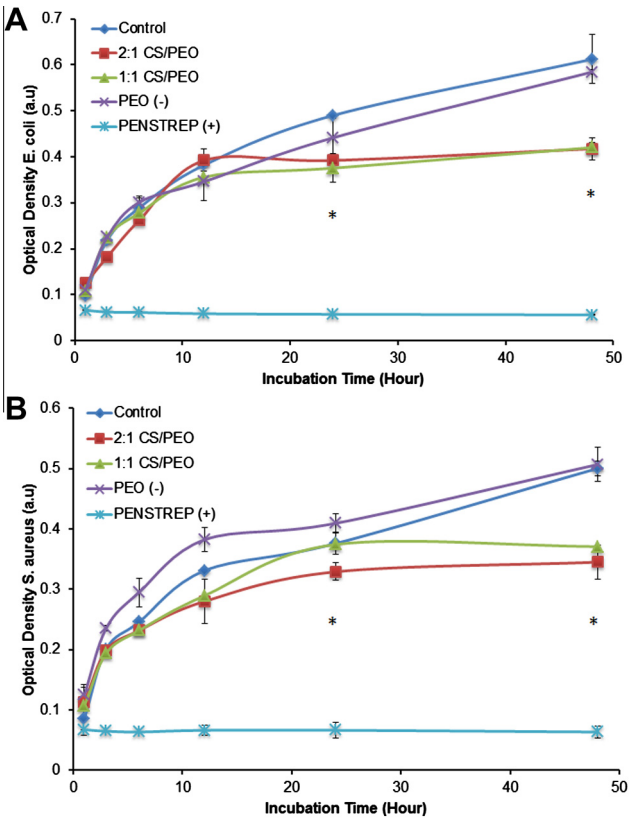


**Fig. 5.** Antibacterial assessment of chitosan/PEO-NP scaffolds compared to negative controls (cell suspension and PEO scaffold) and a positive control (Penstrep solution). 1:1 CS/PEO-NPs and 2:1 CS/PEO-NPs scaffolds showed antibacterial activities against both *E. coli* and *S. aureus* compared to negative controls ($^*p < 0.05$).

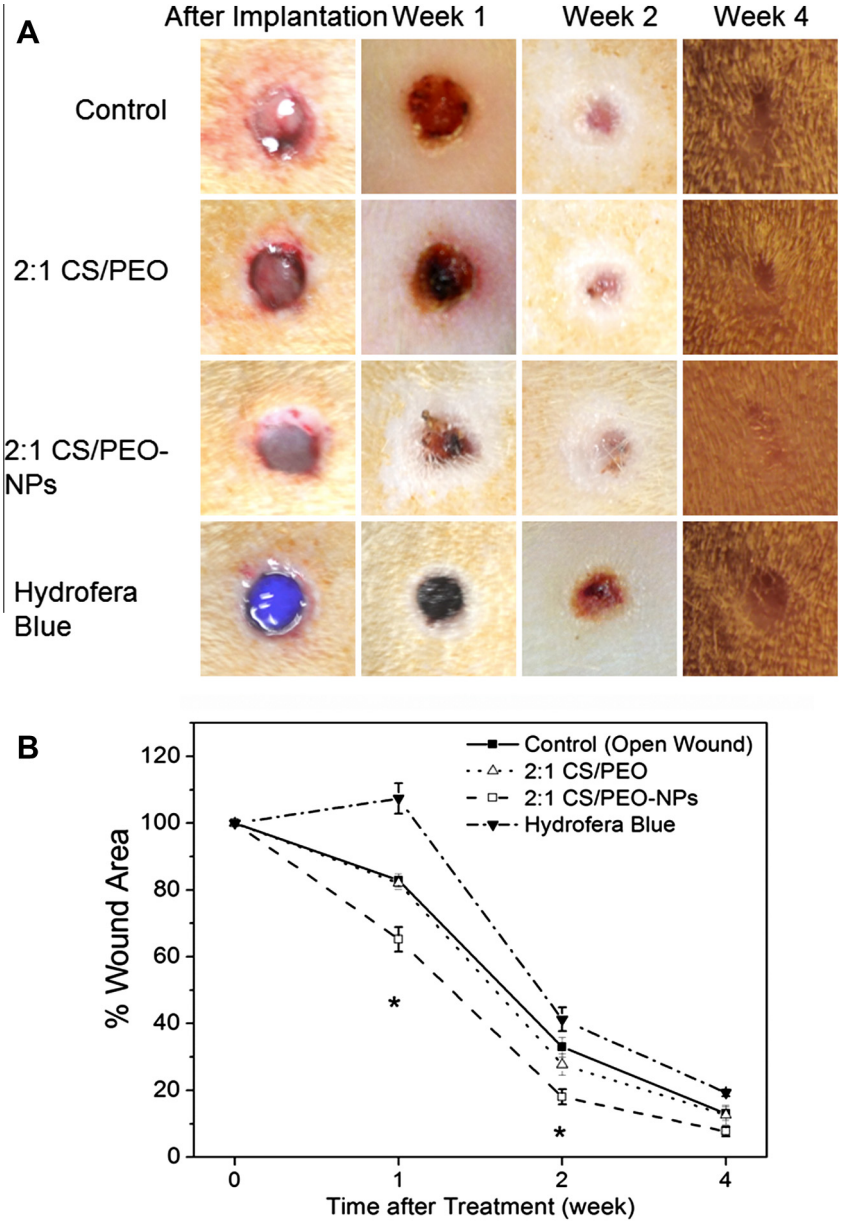


**Fig. 6.** Wound healing evaluation using a full skin rat wound model. (A) Representative macroscopic appearance of wound closure at 0, 1, 2, and 4 weeks after treatment of skin wound of control, 2:1 CS/PEO, 2:1 CS/PEO-NPs, and Hydrofera Blue after 0, 1, 2, and 4 weeks; (B) quantitative measurement of wound size reduction (*$p < 0.01$).

nanoparticles within a CS/PEO-NPs scaffold showed a small initial burst release of 28% at 2 h. In addition, PDGF-BB release from PLGA nanoparticles in fibrous meshes exhibited a sustained release pattern after that (40% at day 7). It is clear that a significant difference can be observed for VEGF release from the nanofiber itself vs. PDGF-BB from nanoparticles within nanofibers (Fig. 3). For wound healing applications, we assume that VEGF could promote angiogenesis at the wound site at early times, thus a fast release of VEGF is desired. We loaded the first growth factor, VEGF, within nanofibers to achieve a fast release. On the other hand, the second growth factor, PDGF-BB, was encapsulated in PLGA nanoparticles to achieve a relatively slower release profile in order to promote fibroblast growth in a sustained manner. This interesting profile from our unique device can help control different growth factor releases and further achieve better wound healing performance.

### 3.3. In vitro cell proliferation

To determine the cell viability and growth on our fibrous scaffolds, human dermal fibroblasts were seeded onto the meshes and MTS assays were used (Fig. 4). For all days studied, PEO/CS scaffolds were cytocompatible, and more cell growth was observed compared to the control without the scaffold. Cell proliferation was significantly increased in samples of days 5 and 7 on all scaffold types compared to the control. An 116.9 ± 2.9% growth was observed on 1:1 CS/PEO on day 5, which is similar to the 115.2 ± 2.8% growth observed on the 2:1 CS/PEO scaffold. Day 7 showed no significant difference between these two samples (as the 1:1 CS/PEO scaffold's 132.6 ± 1.8% compared to the 132.5 ± 2.9% proliferation on 2:1 CS/PEO scaffold). This result suggested that chitosan content is not a major factor to affect fibroblast growth. More importantly, a 2:1 CS/PEO-NPs sample

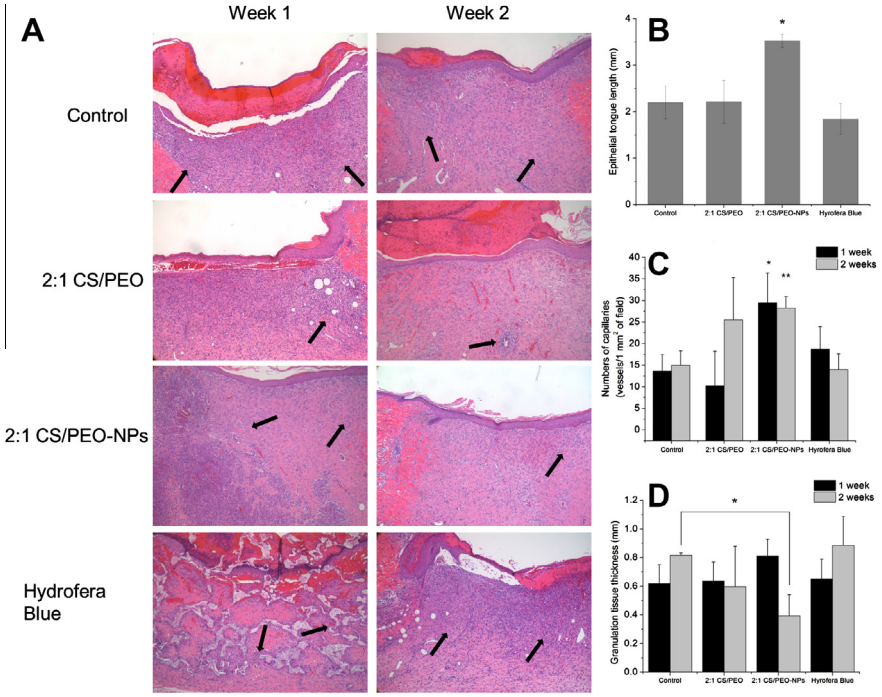


**Fig. 7.** Histological evaluation of wounds treated by CS/PEO-NP meshes. (A) H&E staining for skin wound samples of control (open wound), 2:1 CS/PEO, 2:1 CS/PEO-NPs, Hydrofera Blue after 1 and 2 weeks of treatment; inflammatory cells were indicated by arrows; (B) epithelial length after 1 week of treatment; (C) capillary density at wound site after 1 and 2 weeks of treatment; and (D) granulation tissue thickness after 1 and 2 weeks of treatment. ($^{*}p < 0.05$, $^{**}p < 0.01$).

with PDGF-BB loaded nanoparticles exhibited significantly faster cell growth (140.9 ± 0.8% for day 5 and 156.8 ± 6.6% for day 7) compared to tissue culture plate control and scaffolds without growth factors. Growth factors have been shown to promote fibroblast growth by other studies [39]. Compared to free PDGF-BB added into the growth media, the average cell number on the 2:1 CS/PEO-NPs sample was higher, especially for days 5 and 7. It was ascribed to the larger surface areas provided by the nanofibers, while HDFa cells could grow confluent and thus may stop growing on the TCP. However, no statistically significant difference was observed for fibroblast proliferation with free PDGF-BB or released PDGF-BB, suggesting that the released PDGF-BB preserved its bioactivity. These findings indicated that nanofibrous meshes are cytocompatible and able to provide sustained releases of bioactive growth factors to support dermal fibroblast growth in vitro.

### 3.4. Anti-bacterial property

Bacterial optical density was performed to assess the antibacterial activity of our scaffolds. Two types of bacteria, *E. coli* and *S. aureus*, were chosen. Existing literature has already revealed that chitosan exhibits anti-bacterial behavior [26]. As displayed in Fig. 5, bacteria suspension and PEO only nanofibers showed continuous expansion of both *E. coli* and *S. aureus*. With the incorporation of chitosan in the system, the CS/PEO scaffolds cultured with *E. coli* were shown to have their antibacterial effect by 10 h of culture. Similarly, the same trend was observed when *S. aureus* bacteria grew until the 8 h of culturing, where the scaffold exhibited bacterial inhibiting activity. Penicillin/streptomycin as a positive control was shown to kill all bacteria in solution. The higher amount of CS in 2:1 CS/PEO did have a significantly higher antibacterial effect compared to 1:1 CS/PEO. Thus, CS/PEO composite nanofibers could reduce bacterial growth, leading to the potential inhibition of infection.

### 3.5. In vivo wound healing evaluation

To evaluate the in vivo performance of our dual growth factor-releasing meshes, full thickness skin wounds were created on the back of rats. The gross appearance of each wound was observed after 1, 2, and 4 weeks of treatment (Fig. 6). Electrospun 2:1 CS/PEO nanofiber scaffolds without any growth factor and 2:1 CS/PEO-NPs with VEGF in fibers and PDGF-BB in PLGA nanoparticles were placed and adhered on the wound site easily. Compared to commercial Hyrofera Blue, which requires biological adhesives to get fixed on the wound site, our composite meshes are much easier to attach on wounds. Since PEO is a water-soluble polymer, all electrospun meshes helped the wound stay hydrated, and after ~4 h, they became invisible. The rate of wound closure as a function of time is shown in Fig. 6B, wound area for 2:1 CS/PEO-NPs samples with growth factors is significantly smaller than those of other samples at week 1 and 2 ($p < 0.05$), while 2:1 CS/PEO without growth factors is almost the same as open wound control. It is also noticed that at week 1, Hydrofera Blue had a slightly increased wound size due to the extensive scar formation. After 4 weeks of treatment, all wounds are closed; however, 2:1 CS/PEO-NPs exhibited the smallest scar formation and more hair coverage due to the faster healing process.

The representative macroscopic observations of each wound at 1, 2 and 4 weeks after implantation are shown in Fig. 6A. Throughout the healing process, no infection was observed for all samples. At week 1 of treatment, more granulation and regenerated epidermis were observed for 2:1 CS/PEO-NPs, as confirmed later by histological analysis. Starting from week 1 to week 4, the dual growth factor-releasing composite scaffold did show faster contraction compared to the open wound control and other samples, indicating the effect of the fibrous scaffold and the delivery of PDGF-BB for promoting ECM production. Wound contraction can make the re-epithelialization easier [2]. At week 2 of treatment (Fig. 6A), scab fell off from the skin wound for all samples. Again, 2:1

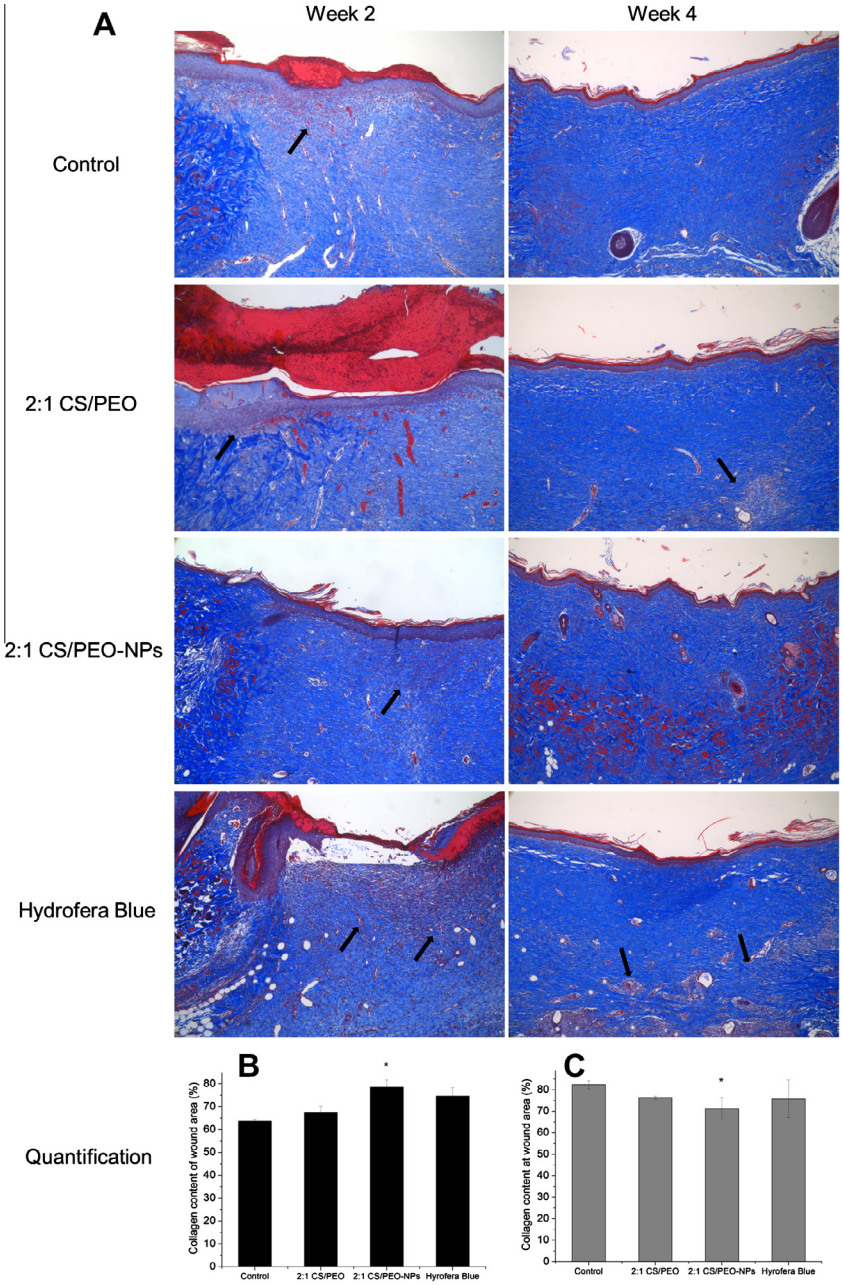


**Fig. 8.** Collagen staining images and quantification of wounds treated by CS/PEO-NP meshes. (A) Masson's Trichrome staining of each wound samples: control, 2:1 CS/PEO, 2:1 CS/PEO-NPs, and Hydrofera Blue at 2 and 4 weeks of treatment; inflammatory cells were indicated by arrows; collagen quantification of each wound area at 2 (B) and 4 (C) weeks of treatment ($^{*}p < 0.05$).

CS/PEO-NPs samples exhibited a faster healing with more regenerated skin and more hair growth. Hydrofera Blue treatment gave the slowest healing rate, probably due to the slow absorption of the material, which is polyvinyl alcohol (PVA). After 4 weeks of treatment (Fig. 6A), all wounds appeared to be closed. Scab was observed on Hydrofera Blue samples only, whereas the wound treated with our VEGF and PDGF-BB releasing fiber meshes obtained almost complete remodeling and hair coverage. Traditionally, increasing growth factor activity could lead to scar formation [40,41]. However, no scar formation was observed in our study, possibly due to the well-controlled release of GFs.

### 3.6. Histological analysis of the wound site

To assess the efficacy of nanofibrous composites in vivo, H&E (Fig. 7) and Masson's Trichrome (Fig. 8) staining were performed on sectioned tissue samples of the wound site. Fig. 7A shows H&E staining of the wound sites at 1 and 2 weeks of treatment. Longer epithelial tongues were also observed on 2:1 CS/PEO-NPs samples, suggesting our GF releasing meshes helped facilitate the epithelium regeneration in the short term (Fig. 7B). At 1 week, significantly more newly formed capillaries were shown for 2:1 CS/PEO-NPs within the wound site compared to open wound ($p < 0.01$), and scaffold without GFs (Fig. 7C). This is expected due to the fast release of VEGF, which had been proven capable of promoting angiogenesis [19,42]. After 2 weeks of treatment, full coverage of new epithelium was identified for all samples except the Hydrofera Blue. Fast creeping of epithelium is also another indicator of faster skin healing post-wounding [43]. In addition, granulation tissue appeared slightly thicker for 2:1 CS/PEO-NPs compared to the Hydrofera Blue and open wound for the 1 week time point (Fig. 7D); however, no significant difference was observed

($p > 0.05$). The thicker granulation tissue was probably formed by the inflammatory response to CS/PEO fibers and PLGA nanoparticles. The commercialized Hydrofera Blue sample showed a less uniform healing response as observing the scaffold material present at the wound bed. At week 2 of treatment, more capillaries also presented for 2:1 CS/PEO-NPs (Fig. 7C). With a complete closure of epithelium, fast clearance of PEO and sustained releasing PDGF-BB, the granulation tissue thickness for 2:1 CS/PEO-NPs at week 2 is significantly reduced compared to that of week 1 and open wound control ($p < 0.01$), suggesting a transition from Phase I (inflammation) to Phase II (proliferation) of the healing process (Fig. 7D). It is also clear that some of the inflammatory cells were replaced by fibroblasts. Since control and Hydrofera Blue still exhibited thicker layers of granulation, they fell behind our GF releasing nanofibers in terms of the healing process.

Masson's Trichrome staining (Fig. 8) was performed to assess the collagen deposition (blue) in the wound site. 2:1 CS/PEO showed a significantly ($p < 0.05$) higher amount of collagen deposition followed by the Hydrofera Blue at 2 weeks of treatment (Fig. 8B). A higher amount of myofibroblast formation at the wound site was identified in the 2:1 CS/PEO-NPs scaffold compared to that of the open wound. Compared to open wound control and nanofibers without GFs, more mature collagen fibers were also observed for 2:1 CS/PEO-NPs sample with less inflammatory cell presence, which is consistent with H&E staining results. More collagen tissue could help in the reconstruction of ECM and further support skin tissue growth [44]. However, after 4 weeks of treatment (Fig. 8C), our GFs releasing nanofibers gave the lowest collagen content at the wound area, and this might be due to more mature collagen formation and more hair follicles regenerated. This morphology indicates that a remodeling phase was already reached for 2:1 CS/PEO-NPs at 4 weeks, while other samples still remained at the tissue regeneration phase with more collagen synthesized and some remaining infiltrated inflammatory cells. It is clear that ECM similar to normal skin was already formed for 2:1 CS/PEO-NPs and the wound area was in transition to regain normal skin functionalities [45]. Indeed, with the help of fast releasing VEGF and slow releasing PDGF-BB, the healing process was promoted by our nanoparticle/nanofiber complex. Compared to traditional growth factor therapy [46,47], our nanofiber/nanoparticles complex provide not only a synergistic delivery of growth factors, but also an ECM mimicry and anti-infection fibrous structure to support the healing process. Thus, our novel composite material could be a promising candidate for ideal wound healing applications as an "all-in-one" set-up.

## 4. Conclusions

A biomimetic nanofibrous scaffold containing nanoparticles was successfully developed with the functionality to release two different growth factors in a relayed manner (fast and sustained release at various phases). The nanofibrous mesh was able to promote fibroblast growth and inhibit bacteria in vitro. With designed quick releasing of VEGF and slow expelling of PDGF-BB, an accelerated wound healing was achieved on a full thickness rat skin wound model. VEGF helped angiogenesis in an early stage of the healing process, while PDGF-BB improved the epithelium regeneration, collagen deposition and functional tissue remodeling. Thus, our dual growth factor releasing device has promising potential in the treatment of chronic complex wounds, for example, diabetic ulcers, in the future.

## Acknowledgements

The authors appreciate the funding support from ARP (Norman Hackerman Advanced Research Program (to K.N.), a National Science Foundation (NSF) Early CAREER Award DMR 1313553 (to J.Y.) NSF CMMI 1266116 (to J.Y.), a National Natural Sciences Foundation of China (NSFC) grant (31228007) (to J.Y.), and a National Institute of Health (NIH) R01 Award EB012575 (to J.Y.). We would also like to acknowledge Dr. Young-Tae Kim for his kind support with the electrospinning apparatus, Dr. John M. Shelton for his help in histological analysis and Miss Alicia J. Sisemore for her help in editing this paper.

## Appendix A. Figures with essential colour discrimination

Certain figures in this article, particularly Figs. 1, 2, 5–8, are difficult to interpret in black and white. The full colour images can be found in the on-line version, at http://dx.doi.org/10.1016/j.actbio.2013.07.030.

## References

[1] Singer AJ, Clark RAF. Cutaneous wound healing. N Engl J Med 1999;341:738–46.
[2] Martin P. Wound healing – aiming for perfect skin regeneration. Science 1997;276:75–81.
[3] Branski LK, Gauglitz GG, Herndon DN, Jeschke MG. A review of gene and stem cell therapy in cutaneous wound healing. Burns 2009;35:171–80.
[4] Boateng JS, Matthews KH, Stevens HN, Eccleston GM. Wound healing dressings and drug delivery systems: a review. J Pharm Sci 2008;97:2892–923.
[5] Zhong SP, Zhang YZ, Lim CT. Tissue scaffolds for skin wound healing and dermal reconstruction. Wiley Interdiscip Rev Nanomed Nanobiotechnol 2010;2:510–25.
[6] Slaughter BV, Khurshid SS, Fisher OZ, Khademhosseini A, Peppas NA. Hydrogels in regenerative medicine. Adv Mater (Deerfield Beach, Fla) 2009;21:3307–29.
[7] Lee KY, Mooney DJ. Hydrogels for tissue engineering. Chem Rev 2001;101:1869–79.
[8] Yildirimer L, Thanh NT, Seifalian AM. Skin regeneration scaffolds: a multimodal bottom-up approach. Trends Biotechnol 2012;30:638–48.
[9] Pierce GF, Mustoe TA. Pharmacologic enhancement of wound healing. Annu Rev Med 1995;46:467–81.
[10] Obara K, Ishihara M, Ishizuka T, Fujita M, Ozeki Y, Maehara T, et al. Photocrosslinkable chitosan hydrogel containing fibroblast growth factor-2 stimulates wound healing in healing-impaired db/db mice. Biomaterials 2003;24:3437–44.
[11] Robson MC, Phillips LG, Robson LE, Thomason A, Pierce GF. Platelet-derived growth factor BB for the treatment of chronic pressure ulcers. Lancet 1992;339:23–5.
[12] Schultz GS, Sibbald RG, Falanga V, Ayello EA, Dowsett C, Harding K, et al. Wound bed preparation: a systematic approach to wound management. Wound Repair Regen 2003;11:S1–S28.
[13] Jain R, Agarwal A, Kierski PR, Schurr MJ, Murphy CJ, McAnulty JF, et al. The use of native chemical functional groups presented by wound beds for the covalent attachment of polymeric microcarriers of bioactive factors. Biomaterials 2013;34:340–52.
[14] Yang Y, Xia T, Zhi W, Wei L, Weng J, Zhang C, et al. Promotion of skin regeneration in diabetic rats by electrospun core-sheath fibers loaded with basic fibroblast growth factor. Biomaterials 2011;32:4243–54.
[15] Yang Y, Xia T, Chen F, Wei W, Liu C, He S, et al. Electrospun fibers with plasmid bFGF polyplex loadings promote skin wound healing in diabetic rats. Mol Pharm 2012;9:48–58.
[16] Choi JS, Leong KW, Yoo HS. In vivo wound healing of diabetic ulcers using electrospun nanofibers immobilized with human epidermal growth factor (EGF). Biomaterials 2008;29:587–96.
[17] Liu X, Lin T, Fang J, Yao G, Zhao H, Dodson M, et al. In vivo wound healing and antibacterial performances of electrospun nanofibre membranes. J Biomed Mater Res, Part A 2010;94:499–508.
[18] Chandrasekaran AR, Venugopal J, Sundarrajan S, Ramakrishna S. Fabrication of a nanofibrous scaffold with improved bioactivity for culture of human dermal fibroblasts for skin regeneration. Biomed Mater (Bristol, England) 2011;6:015001.
[19] Ackermann M, Wolloscheck T, Wellmann A, Li VW, Li WW, Konerding MA. Priming with a combination of proangiogenic growth factors enhances wound healing in streptozotocin-induced diabetes in mice. Eur Surg Res 2011;47:81–9.
[20] Ackermann M, Wolloscheck T, Wellmann A, Li VW, Li WW, Konerding MA. Priming with a combination of proangiogenic growth factors improves wound healing in normoglycemic mice. Int J Mol Med 2011;27:647–53.
[21] Barrientos S, Stojadinovic O, Golinko MS, Brem H, Tomic-Canic M. Growth factors and cytokines in wound healing. Wound Repair Regen 2008;16:585–601.
[22] Li J, Zhang Y-P, Kirsner RS. Angiogenesis in wound repair: angiogenic growth factors and the extracellular matrix. Microsc Res Tech 2003;60:107–14.

[23] Rujitanaroj P-O, Pimpha N, Supaphol P. Wound-dressing materials with antibacterial activity from electrospun gelatin fiber mats containing silver nanoparticles. Polymer 2008;49:4723–32.
[24] Elsner JJ, Zilberman M. Antibiotic-eluting bioresorbable composite fibers for wound healing applications: microstructure, drug delivery and mechanical properties. Acta Biomater 2009;5:2872–83.
[25] Katti DS, Robinson KW, Ko FK, Laurencin CT. Bioresorbable nanofiber-based systems for wound healing and drug delivery: optimization of fabrication parameters. J Biomed Mater Res B Appl Biomater 2004;70:286–96.
[26] Rabea EI, Badawy MET, Stevens CV, Smagghe G, Steurbaut W. Chitosan as antimicrobial agent: applications and mode of action. Biomacromolecules 2003;4:1457–65.
[27] Menon JU, Kona S, Wadajkar AS, Desai F, Vadla A, Nguyen KT. Effects of surfactants on the properties of PLGA nanoparticles. J Biomed Mater Res, Part A 2012;100:1998–2005.
[28] Rho KS, Jeong L, Lee G, Seo BM, Park YJ, Hong SD, et al. Electrospinning of collagen nanofibers: effects on the behavior of normal human keratinocytes and early-stage wound healing. Biomaterials 2006;27:1452–61.
[29] Lee J, Yoo JJ, Atala A, Lee SJ. The effect of controlled release of PDGF-BB from heparin-conjugated electrospun PCL/gelatin scaffolds on cellular bioactivity and infiltration. Biomaterials 2012;33:6709–20.
[30] Sahoo S, Ang LT, Goh JC, Toh SL. Growth factor delivery through electrospun nanofibers in scaffolds for tissue engineering applications. J Biomed Mater Res, Part A 2010;93:1539–50.
[31] Wang Y, Wang B, Qiao W, Yin T. A novel controlled release drug delivery system for multiple drugs based on electrospun nanofibers containing nanoparticles. J Pharm Sci 2010;99:4805–11.
[32] Mickova A, Buzgo M, Benada O, Rampichova M, Fisar Z, Filova E, et al. Core/shell nanofibers with embedded liposomes as a drug delivery system. Biomacromolecules 2012;13:952–62.
[33] Greiner A, Wendorff JH. Electrospinning: a fascinating method for the preparation of ultrathin fibers. Angew Chem Int Ed 2007;46:5670–703.
[34] Jin W-J, Lee HK, Jeong EH, Park WH, Youk JH. Preparation of polymer nanofibers containing silver nanoparticles by using poly(N-vinylpyrrolidone). Macromol Rapid Commun 2005;26:1903–7.
[35] Agarwal A, Nelson TB, Kierski PR, Schurr MJ, Murphy CJ, Czuprynski CJ, et al. Polymeric multilayers that localize the release of chlorhexidine from biologic wound dressings. Biomaterials 2012;33:6783–92.
[36] Su X, Kim B-S, Kim SR, Hammond PT, Irvine DJ. Layer-by-layer-assembled multilayer films for transcutaneous drug and vaccine delivery. ACS Nano 2009;3:3719–29.
[37] Nguyen TT, Ghosh C, Hwang SG, Chanunpanich N, Park JS. Porous core/sheath composite nanofibers fabricated by coaxial electrospinning as a potential mat for drug release system. Int J Pharm 2012;439:296–306.
[38] Wood KC, Chuang HF, Batten RD, Lynn DM, Hammond PT. Controlling interlayer diffusion to achieve sustained, multiagent delivery from layer-by-layer thin films. Proc Natl Acad Sci USA 2006;103:10207–12.
[39] Pierce GF, Tarpley JE, Yanagihara D, Mustoe TA, Fox GM, Thomason A. Platelet-derived growth factor (BB homodimer), transforming growth factor-beta 1 and basic fibroblast growth factor in dermal wound healing. Neovessel and matrix formation and cessation of repair. Am J Pathol 1992;140:1375–88.
[40] Wilgus TA, Ferreira AM, Oberyszyn TM, Bergdall VK, Dipietro LA. Regulation of scar formation by vascular endothelial growth factor. Lab Invest 2008;88:579–90.
[41] Krein PM, Huang Y, Winston BW. Growth factor regulation and manipulation in wound repair: to scar or not to scar, that is the question. Expert Opin Ther Pat 2001;11:1065–79.
[42] Frank S, Hubner G, Breier G, Longaker MT, Greenhalgh DG, Werner S. Regulation of vascular endothelial growth factor expression in cultured keratinocytes: implications for normal and impaired wound healing. J Biol Chem 1995;270:12607–13.
[43] Li P, Liu P, Xiong RP, Chen XY, Zhao Y, Lu WP, et al. Ski, a modulator of wound healing and scar formation in the rat skin and rabbit ear. J Pathol 2011;223:659–71.
[44] Sung JH, Hwang MR, Kim JO, Lee JH, Kim YI, Kim JH, et al. Gel characterisation and in vivo evaluation of minocycline-loaded wound dressing with enhanced wound healing using polyvinyl alcohol and chitosan. Int J Pharm 2010;392:232–40.
[45] Owens P, Engelking E, Han G, Haeger SM, Wang XJ. Epidermal Smad4 deletion results in aberrant wound healing. Am J Pathol 2010;176:122–33.
[46] Brown RL, Breeden MP, Greenhalgh DG. PDGF and TGF-α act synergistically to improve wound healing in the genetically diabetic mouse. J Surg Res 1994;56:562–70.
[47] Greenhalgh DG, Sprugel KH, Murray MJ, Ross R. PDGF and FGF stimulate wound healing in the genetically diabetic mouse. Am J Pathol 1990;136:1235–46.